Supplementary Material

FEED-FORWARD INHIBITION CONTROLS THE SPREAD OF GRANULE CELL INDUCED PURKINJE CELL ACTIVITY IN THE CEREBELLAR CORTEX

Fidel Santamaria[1]*, Patrick G. Tripp[3], and James M. Bower[2,3]

[1]Computation and Neural Systems Program, California Institute of Technology 216-76 Pasadena, CA 91125.

[2]Research Imaging Center, University of Texas Health Science Center at San Antonio and [3]Cajal Neuroscience Research Center at the University of Texas San Antonio, 7703 Floyd Curl Drive, San Antonio, TX 78284-6240, bower@uthscsa.edu

* Present address: Dept. of Neurobiology, P.O. Box 3209, Duke University Medical Center. santamaria@neuro.duke.edu.

METHODS

Purkinje cell model

The following dendritic ionic channels were implemented in the Purkinje cell (PC) model: two types of Ca channels, a P-type, CaP (Llinas et al., 1989) and a T-type, CaT (Kaneda et al., 1990); two types of Ca-activated K+ channels (Kca), a BK-type, BK (Latorre et al., 1989) and a K2-type, K2 (Gruol et al., 1991); and a persistent K+ channel. The soma had two types of sodium channels, a fast current, NaF (Hirano and Hagiwara, 1989) and a slow persistent current, NaP (French et al., 1990); one type of calcium current T-type; and four types of potassium channels, anomalous rectifier, Kh (Spain et al., 1987); delayed rectifier, Kdr (Yamada et al., 1989); persistent potassium, Km (Yamada et al., 1989); and an A-type, KA (Hirano and Hagiwara, 1989). The ion channels had the following conductance function (De Schutter and Bower, 1994a):

$$G(V,[Ca^{2+}]_i,t) = \bar{g}m(V,t)^n h(V,t)^q z([Ca^{2+}]_i,t)^r$$

The gates *m* and *h* were calculated using:

$\frac{\partial m}{\partial t} = \alpha_m(1-m) - \beta_m m,$ same for h.

$$\alpha m(V,t) = \frac{A}{B + e^{(V+C)/D}}, \quad \beta_m(V,t) = \frac{E}{F + e^{(V+B)/H}}$$

and for the activation rates of the $[Ca^{2+}]_i$ dependent gates:

$$\frac{\partial z}{\partial t} = \frac{z_\infty - z}{\tau_z}, \quad z_\infty = \frac{1}{1 + \frac{A}{[Ca^{2+}]_i}}, \quad \tau_z = B$$

Refer to Table S1 for parameter values for each current.

The ionic channels were distributed over three zones of the model, with Na channels in the soma, fast K channels in the soma and main dendrite, and Ca channels and Ca-activated K channels in the entire dendrite. Previously published results have shown that the model's responses to current injection are robust to changes in densities of all of the ionic channels (De Schutter and Bower, 1994a). Modifying densities by factors >=2 result in left or right shifts of the frequency-current curve. However, changes of >20% to the amount of P-type Ca channels of one of the Ca-activated K channels in the model either suppressed dendritic spikes or cause the model to always fire Ca spikes (De Schutter and Bower, 1994a).

Although our model did not include a strong resurgent Na+ current (Afshari et al., 2004) it was able to replicate appropriately the relevant experimental results.

Experimental procedures

Animals were initially anesthetized with halothane and given an intraperitoneal (IP) injection of ketamine-xylazine-acepromazine (ketamine 100mg/kg; xylazine 5 mg/kg; acepromazine 1mg/kg). Supplemental doses (20% of initial dose) were given IP as needed throughout the experiment to maintain deep anesthesia as evidenced by the lack of a pinch withdrawal reflex and/or lack of whisking. Body temperature was maintained at 36±1 °C with the use of a rectal temperature probe and heating pad. To maintain proper hydration, 0.9 ml of lactated Ringer's solution was injected IP every 1-2 hours. Animals were euthanized at the end of the experiment with a 1.0 ml intracardiac injection of Nembutal. The techniques to expose the cerebellar cortex for recordings were identical to those used by

Brown and Bower (2001).

Recording depths were restricted to between 300 and 500 μm below the cortical surface to assure that only PCs in the superficial region of Crus IIa were recorded, and that all isolated PCs were in line with respect to parallel fiber (pf) activation.

Recorded electrical signals were amplified 1,000 times (BAK, Maryland; and A-M systems, Washington), and filtered between 500 Hz and 5 kHz. PC responses were isolated using a custom made spike sorting algorithm (LabView-National Instruments, TX) based on different discrimination windows evaluating the stability of voltage before a spike; spike height; the valley of the spike; and stable voltage after the spike. The discrimination window never exceeded two milliseconds. Once the timing of individual spikes in each train was determined, dot rasters and peri-stimulus time histograms (PSTHs) were generated. Proper spike discrimination was checked by evaluating inter spike interval histograms (ISIH). In all experiments we recorded action potentials from PCs identified based on their characteristic firing rate (average 40 Hz), inter-spike interval histogram, depth of recording electrode in the molecular layer, and the presence of complex climbing fiber type responses (Bower and Woolston, 1983). We monitored changes in PC responses waveforms before and after topical application of the GABA-A antagonist bicuculline.

RESULTS

Scaling of pf number and firing frequency

In the network model we implemented ~1% of the total number of granule cells

that make a synaptic contact with an individual PC (1,600 out of 150,000, Harvey and Napper, 1991). We compensated for this reduced number of excitatory synapses by proportionally increasing their firing rate. Assuming non-saturating synaptic input, the total conductance onto the PC model is $f*N*a$. Where f is the frequency, N is the number of synapses, and a is the maximum conductance of a single synapse. Therefore, the frequency needed to keep the total conductance constant while increasing the number of synapses is given by $f_n=f*N*a/(N_n*a)$. With 1,600 pfs a 4 Hz granule cell background average firing rate was needed to maintain physiologically realistic levels of spontaneous PC activity, therefore, with 15,000 pfs the average firing rate of each granule cell was reduced to 0.43 Hz. In agreement with this prediction the PSTHs shown in Figure S1 were obtained from a modeled PC receiving activity from 15,000 pfs with an average background firing rate of 0.47 Hz. This level of input resulted in a background firing rate close to 40 Hz, and a physiologically realistic spatial pattern of PC responses following simulated granule cell layer stimulation, which is similar to that obtained in the model with 1,600 pfs firing at 4 Hz (Figure 3 in the primary paper). Similar scaling tests were not necessary with respect to the number of inhibitory synapses as the simulated number of synapses was in the range of those found *in vivo*.

Robustness of the results with respect to pf propagation velocities

As discussed in the main text, the data presented in the figures were obtained using the widest range of pf propagation velocities reported in mammals. These values were chosen to provide the most rigorous test of the desynchronization

hypothesis. In addition to simulating a larger number of pfs, the data shown in Figure S1 was also obtained using the slower pf conduction velocities specifically reported for rats 0.2-0.27 m/s (Vranesic et al., 1994). The effects on network behavior are shown in more detail in Figure S2 where the more narrower range of propagation velocities (and less desynchornization) are shown in A, simulated changes in PC firing frequencies are shown in B, the number of required basket-type synapses and their temporal delays are shown in C and D respectively, and the same data is shown for stellate-type inhibition in E and F. Again, as in the main paper, the different symbols indicate variations in these parameters in different simulation runs. Both Figures S1 and S2 show that the model replicates the spatial and temporal pattern of PC responses to granule cell layer activation, even when the conduction velocity of pfs are adjusted to correspond to those reported in the rat (Vranesic et al., 1994).

Summary of model parameters

Table S2 is a summary of the parameters used to set up the network simulations. The table shows the ranges of values that we explored for granule cell numbers, inhibitory interneurons synapses, synaptic kinetics, propagation velocities, and connectivity patterns. When available, the references for the values used for each parameter are indicated. Similarly, Table S3 shows the range of values of the excitatory and feed-forward inhibitory mechanisms that replicate the experimental results.

REFERENCES

Afshari FS, Ptak K, Khaliq ZM, Grieco TM, Slater NT, McCrimmon DR, Raman IM. Resurgent Na currents in four classes of neurons of the cerebellum. J Neurophysiol. 92(5):2, 2004.

Barbour B. Synaptic Currents Evoked in Purkinje-Cells by Stimulating Individual Granule Cells. Neuron 11:759-769, 1993.

Brown IE, Bower JM. Congruence of mossy fiber and climbing fiber tactile projections in the lateral hemispheres of the rat cerebellum. J Comp Neurol 429:59-70, 2001.

Diana MA, Marty A. Characterization of depolarization-induced suppression of inhibition using paired interneuron--Purkinje cell recordings. J Neurosci 23:5906-5918, 2003.

Farrant M, Cull-Candy SG. Excitatory amino acid receptor-channels in Purkinje cells in thin cerebellar slices. Proc Biol Sci 244:179-184, 1991.

French CR, Sah P, Buckett KJ, Gage PW. A voltage-dependent persistent sodium current in mammalian hippocampal neurons. J Gen Physiol 95:1139-1157, 1990.

Gruol DL, Jacquin T, Yool AJ. Single-channel K+ currents recorded from the somatic and dencritic regions of cerebellar Purkinje neurons in culture. J Neurosci 11:1002-1015, 1991.

Hirano T, Hagiwara S. Kinetics and distribution of voltage-gated Ca, Na and K channels on the somata of rat cerebellar Purkinje cells. Pflugers Arch Eur

J Physiol 413:463-469, 1989.

Kaneda M, Wakamori M, Ito C, Akaike N. Low-threshold calcium current in isolated Purkinje cell bodies of rat cerebellum. Journal of Neurophysiology 63:1046-1051, 1990.

Latorre R, OBerhauser A, Labarca P, Alvarez O. Varieties of calcium-activated potassium channels. Annu Rev Physiol 51:385-399, 1989.

Llinas RR, Sugimori M, Cherksey B. Voltage-dependent calcium conductances in mammalian neurons. The P channel. Ann N Y Acad Sci 560:103-111, 1989.

Rapp M, Segev I, Yarom Y. Physiology, morphology and detailed passive models of guinea-pig cerebellar Purkinje cells. J Physiol 474:101-118, 1994.

Spain WJ, Schwindt PC, Crill WE. Anomalous rectification in neurons from cat sensorimotor cortex in vitro. j Neurophysiol 57:1555-1576, 1987.

Yamada WM, Koch C, Adams PR. Multiple channels and calcium dynamics. In: Methods in neuronal modeling: From synapses to networks (Koch C, Segev I, eds), pp 97-133. Cambridge: MIT Press, 1989.

Table S1

Conductances for the voltage and Ca_{2+} dependent channels in the PC model. Parameters A, F, and H are in mV. For KC and BK factor z is in μM and B in ms.

NAME	***Vr***	***Gate***	***P***	***A***	***B***	***C***	***D***	***E***	***F***	***G***	***H***
NaF	45	m	3	35	0	5	-10	7	0	65	20
		h	1	0.23	1	80	10	7.5	0	-3	-18
NaP	45	m	3	200	1	-18	-16	25	1	58	8
CaP	135	m	1	8.5	1	-8	-12.5	35	1	74	14.5
		h	1	$1.50x10^{-3}$	1	29	8	$5.5x10^{-3}$	1	23	-8
CaT	135	m	1	2.6	1	21	-8	0.18	1	40	4
		h	1	$2.50x10^{-3}$	1	40	8	0.19	1	50	-10
Kh	-30										
Kdr	-85										
KM	-85										
KA	-85	m	4	1.4	1	27	-12	0.49	1	30	4
		h	1	$1.75x10^{-2}$	1	50	8	1.3	1	13	-10
KC	-85	m	1	7.5, α_m is constant				0.11	0	-35	14.9
		z	2	4	10						
K2	-85	m	1	25, α_m is constant				$7.5x10^{-2}$	0	5	10
		z	2	0.2	10						

Table S2

Network parameters used to setup the cerebellar cortex model.

Parameter	***Value***	***Notes and references***
Granule cells	1,600	1% of the actual number (Harvey and Napper, 1991).
Inhibitory synapses	1,695	Within reported range (Sultan and Bower, 1998).
Background activity	Mean 4.0 Hz	Granule cells
	Mean 1.1 Hz	Inhibitory interneuron. All: Randomly activated following a Poisson distribution. Results in 40 Hz PC firing rate (Bower and Woolston, 1983).
Granule cell to PC connectivity	Every 10-90 μm	Ascending segment when on top of site of granule cell stimulation. Spines on dendrites < 1.5 μm diameter.
	1 spine per granule cell	When along the parallel fibers. Spines on dendrites between 1.5-3.15 μm (Gundappa-Sulur et al., 1999)
Excitatory synapses kinetics	0.7 nS amplitude, 0.5 ms opening time, 7.3 ms closing time; 0 mV reversal potential.	Modeled as AMPA synapses (Barbour, 1993).
Inhibitory interneuron to PC connectivity	Randomly distributed over dendrite	Stellate-type over dendritic tree; basket-type on the soma.
Inhibitory synapses kinetics	1.4 mS/cm^2 Stellate-type on smooth dendrites; 7 mS/cm^2 Stellate-type on spiny dendrites; 100 $\mu S/cm^2$ Basket-type on soma.	Modeled as GABA-A synapses (Diana and Marty, 2003). All: 0.9 ms opening time constant, 12.1 ms closing time constant; -80 mV reversal potential
Evoked granule cell activity	0-10 % of all granule cell synapses. Selected in a patch.	From an estimated upper value of 20% (Methods)
Feed-forward inhibition connectivity	Molecular layer divided in three overlapping sections: -100-200 μm; 0-300 μm; and 200-400 μm.	Depth in the molecular layer measured from the position of the PC soma.
Evoked inhibitory interneuron synapses to PC connectivity	Top layer: Stellate-type synapse. Middle and bottom layers: Mixed stellate- and basket-type synapse.	Sub-set of original set of inhibitory synapses chosen at random within each layer. Activation of the synapses is at least 1 ms after the arrival of the first action potential along parallel fibers to each layer.
Parallel fiber propagation velocities	0.20-0.27 m/s.	In rat (Vranesic et al., 1994).
	0.15-0.5 m/s.	Widest reported for all species. (0.15 m/s in rats; Vranesic et al., 1994; 0.5 m/s in cats; Crepel et al., 1981).

Table S3

Range of parameters predicted in the model that suppress a beam of PC excitation after granule cell layer stimulation along the pfs.

Parameter	***Range***	***Notes***
Minimum granule cell layer activation	2% of total number of granule cells	Activates a PC beam along the full length of parallel fibers if not compensated by feed-forward inhibition. Could be smaller when using higher numbers of parallel fibers in the simulation (Figure S1).
Basket cell synapses	1-16	Fast decay as distance increases from site of stimulation.
Stellate cell synapses	0-30	Increasing as a function of the distance to site of stimulation. Not always required on top of stimulation site.
Basket cell synaptic delay	1-5 ms	Shorter as distance increases from site of stimulation.
Stellate cell synaptic delay	1-5 ms	Wide range outside the areas closest to site of stimulation.

FIGURE S1

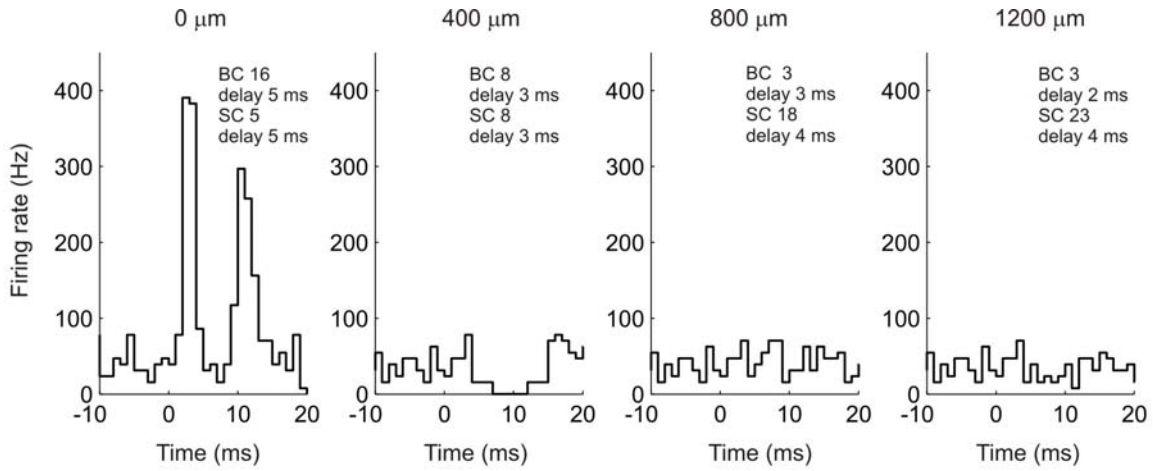

Santamaria et al. Supplementary Figure S1

PSTHs (256 trials) for four PCs at different distances from the site of granule cell stimulation. The network simulation consisted in using 15,000 granule cells, the range of pf conduction velocities found in the rat (0.20 top, 0.27 m/s bottom), and only 0.5% of the granule cells were used for the stimulation. The PC on top of the

site of stimulation received the same total amount of excitatory input, split between ascending and pf synapses. The notations indicate the inhibitory conduction delays as well as the number of basket (BC) and stellate cell (SC) synapses converging on the corresponding PCs. All simulated PCs received randomly activated excitatory (0.47 Hz) and inhibitory (1.1 Hz) synapses resulting in an average spontaneous firing frequency of 40 Hz. Compare to the results shown in Figure 3E-H in the main text.

FIGURE S2

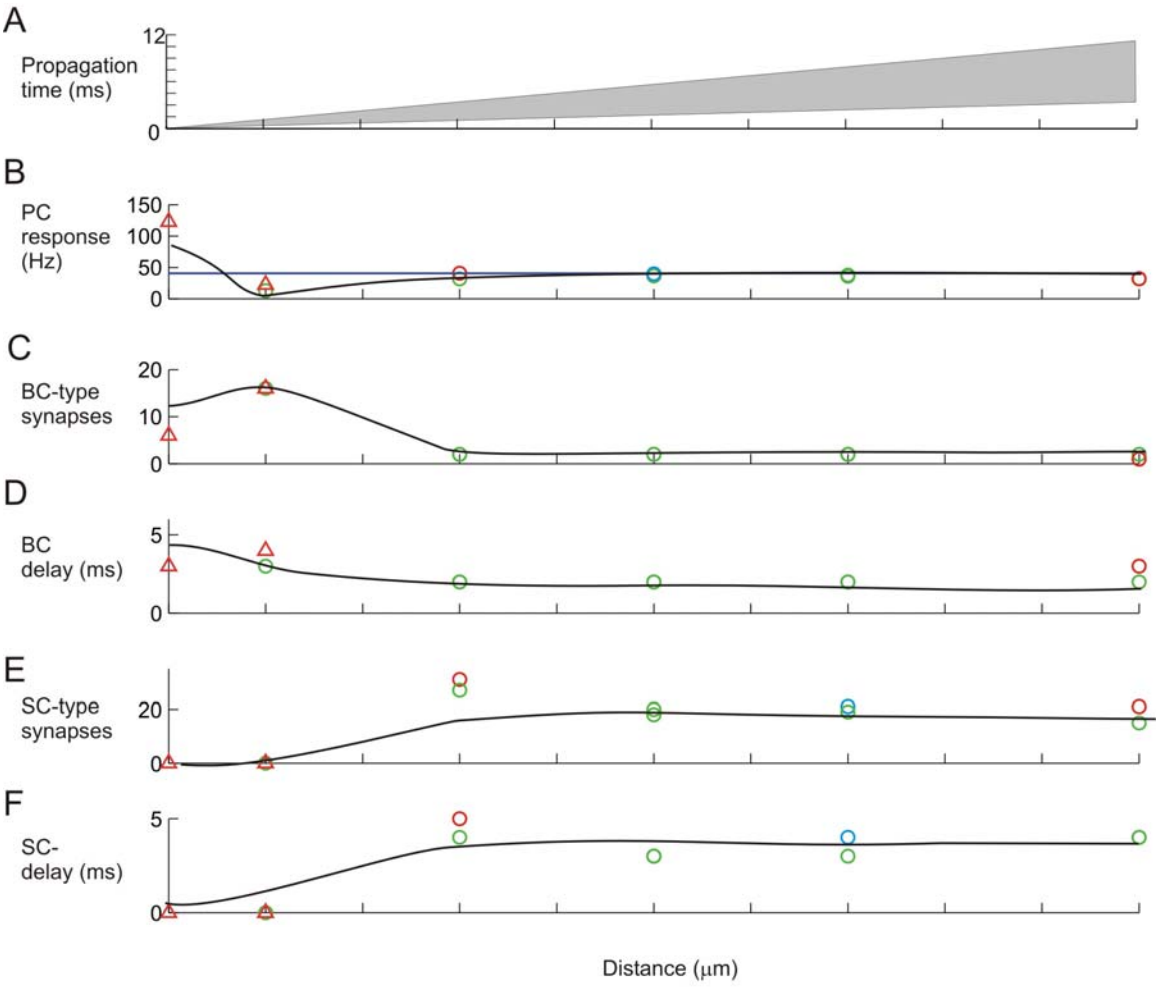

Santamaria, et al. Supplementary Figure S2

Network mechanisms of PC beam suppression predicted by the model using the slower pf propagation velocities found in the rat (0.2-0.27 m/s). A: Narrower predicted desynchronization of the pf volley as a function of distance from the

site of granule cell layer activation. B: Average firing rate 15 ms after arrival of first pf action potential to a PC at different distances from the site of granule cell layer activation. C: Number of basket-type synapses needed to reproduce the experimental results. D: Required temporal delays between pf excitation and activation of feed-forward basket-type inhibition. E: Number of inhibitory stellate-type synapses needed to replicate the experimental data. F: Temporal delay between pf excitation and activation of feed-forward stellate-type inhibition. Different shaped and colored symbols indicate different sets of parameters in different simulation runs. Each simulation consisted in 256 trials.

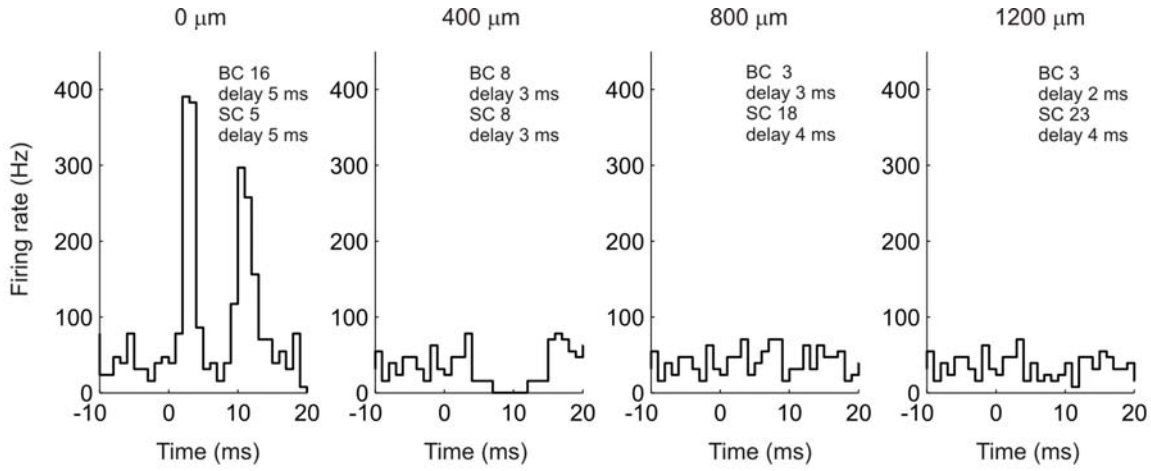

Santamaria et al. Supplementary Figure S1

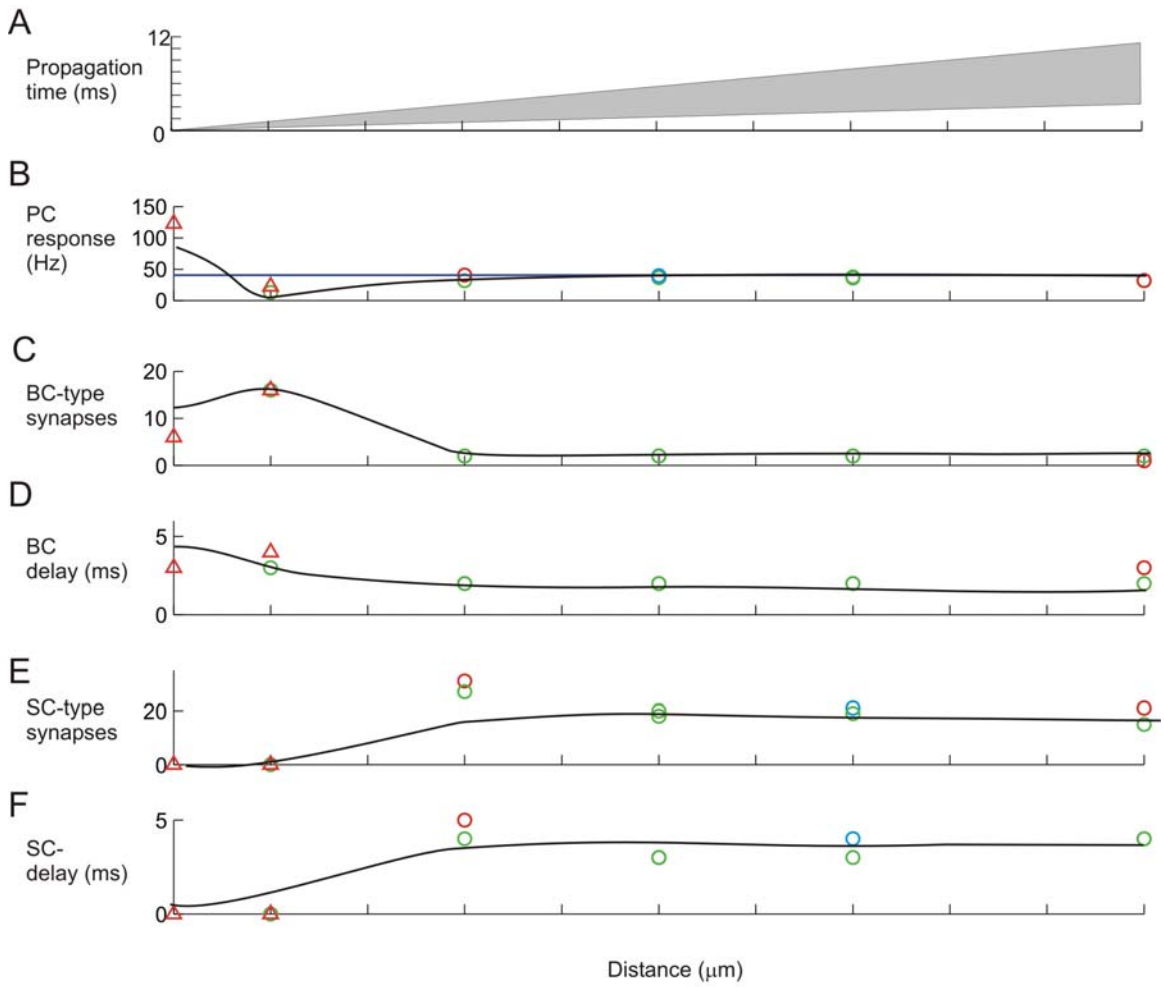

Santamaria, et al. Supplementary Figure S2